J Antimicrob Chemother 2020; **75**: 3260–3268
doi:10.1093/jac/dkaa314 Advance Access publication 11 August 2020

Journal of Antimicrobial Chemotherapy

Characterizing the non-linear pharmacokinetics of miltefosine in paediatric visceral leishmaniasis patients from Eastern Africa

Semra Palić[1], Anke E. Kip[1], Jos H. Beijnen[1], Jane Mbui[2], Ahmed Musa[3], Alexandra Solomos[4], Monique Wasunna[5], Joseph Olobo[6], Fabiana Alves[4] and Thomas P. C. Dorlo [1]*

[1]Department of Pharmacy & Pharmacology, The Netherlands Cancer Institute—Antoni van Leeuwenhoek Hospital, Amsterdam, The Netherlands; [2]Centre for Clinical Research, Kenya Medical Research Institute, Nairobi, Kenya; [3]Institute of Endemic Diseases, University of Khartoum, Khartoum, Sudan; [4]Drugs for Neglected Diseases initiative, Geneva, Switzerland; [5]Drugs for Neglected Diseases initiative, Nairobi, Kenya; [6]Department of Immunology and Molecular Biology, College of Health Sciences, Makerere University, Kampala, Uganda

*Corresponding author. E-mail: t.dorlo@nki.nl

Received 25 September 2019; accepted 7 June 2020

Background: Conventional miltefosine dosing (2.5 mg/kg/day) for treatment of visceral leishmaniasis (VL) is less effective in children than in adults. A higher allometric dose (median 3.2 mg/kg/day) was therefore investigated in paediatric VL patients in Eastern Africa. Results of this trial showed an unforeseen, lower than dose-proportional increase in exposure. Therefore, we performed a pooled model-based analysis of the paediatric data available from both dosing regimens to characterize observed non-linearities in miltefosine pharmacokinetics (PK).

Methods: Fifty-one children with VL were included in this analysis, treated with either a conventional ($n = 21$) or allometric ($n = 30$) miltefosine dosing regimen. PK data were analysed using non-linear mixed-effects modelling.

Results: A two-compartment model following first-order absorption and linear elimination, with two separate effects on relative oral bioavailability, was found to fit these data best. A 69% lower bioavailability at treatment start was estimated, presumably due to initial malnourishment and malabsorption. Stagnation in miltefosine accumulation in plasma, hampering increased drug exposure, was related to the increase in cumulative dose (mg/kg/day). However, the allometric regimen increased exposure 1.7-fold in the first treatment week and reduced the time to reach the PK target by 17.4%.

Conclusions: Miltefosine PK in children suffering from VL are characterized by dose-dependent non-linearities that obstruct the initially expected exposure levels. Bioavailability appeared to be affected by the cumulative dose, possibly as a consequence of impaired absorption. Despite this, allometric dosing led to a faster target achievement and increased exposure compared with conventional dosing.

Introduction

Visceral leishmaniasis (VL) or kala-azar is among the most fatal parasitic diseases.[1] VL is primarily associated with poverty, and is therefore ranked as one of the most neglected tropical infections.[2] Limited treatment options are available for VL, most being hampered by poor or variable efficacy, high toxicity and parenteral routes of administration.[3,4] Miltefosine is an alkylphosphocholine agent, which was originally assessed for treatment of cutaneous metastases in breast cancer but has been repurposed for treatment of leishmanial infections.[5] Today, miltefosine is the only oral drug available for treatment of VL. Miltefosine pharmacokinetics (PK) are characterized by slow absorption and elimination, leading to long initial (approximately 7 days) and terminal (approximately 30 days) half-lives.[6,7] The absorption of miltefosine appears to be concentration dependent, with passive paracellular diffusion applicable to the concentration below 20.4 μg/mL. Above this concentration, saturable mechanisms of absorption have been observed in Caco-2 cells.[8,9]

The first clinical trials of miltefosine for the treatment of VL were conducted in India, where a 28 day treatment with a linear dose of 2.5 mg/kg/day in both children (age 2–11) and adults (older than 15 years of age) resulted in a cure rate of 90% for

© The Author(s) 2020. Published by Oxford University Press on behalf of the British Society for Antimicrobial Chemotherapy.
This is an Open Access article distributed under the terms of the Creative Commons Attribution Non-Commercial License (http://creativecommons.org/licenses/by-nc/4.0/), which permits non-commercial re-use, distribution, and reproduction in any medium, provided the original work is properly cited. For commercial re-use, please contact journals.permissions@oup.com

children and of 97% for adults.[10,11] In a phase II trial in Sudan and Kenya, a conventional 28 day treatment with miltefosine alone resulted in an overall cure rate of 72% at 6 months follow-up.[12] Results from this trial indicated decreased efficacy in patients younger than 12 years (59%) in comparison with patients ≥12 years (86%), with discouraging exposure in children who had a body weight lower than 30 kg, which was reported to be 33% lower than in the adult patient cohort.[12] Previously, in patients from Nepal, the exposure–effect relationship was determined for the time above 90% effective concentration (EC_{90}), indicating that the time that the miltefosine concentration is below the EC_{90} was related to the probability of treatment failure, due to recrudescence of *Leishmania* parasites.[13] The highest probability of treatment success was for 29.5 days >EC_{90} for miltefosine therapy.[14]

With the intention of increasing exposure to miltefosine in the paediatric population, model-based simulations were performed, taking into account the difference in fat-free mass (FFM) between children and adults. Predictions derived from these simulations suggested that administering a relatively higher daily mg/kg (allometric) dose of miltefosine to patients with lower FFM would result in children reaching exposure levels equivalent to those of adult patients.[15] Consequently, an open label clinical trial was conducted in Kenya and Uganda with this new allometric dosing regimen.[15] The main goal of this trial was to increase exposure to miltefosine in Eastern African children, ultimately improving treatment outcomes. Efficacy in the 30 children with VL (aged 4–12 years) treated with a 28 day allometric miltefosine regimen was indeed increased to 90% at 6 months follow-up.[16] However, the results showed an unexpected less than dose-proportional increase in exposure during treatment [AUC from days 0 to 28 (AUC_{d0-28})]. In 40% of the observed PK profiles, accumulation of miltefosine in plasma stagnated in the third week of treatment. We have now performed a pooled model-based analysis of the Eastern African paediatric PK data from both the conventional and allometric dose regimens, with the aim of characterizing and elucidating the non-linearities in miltefosine PK observed in children treated for VL.

Methods

Patient population

Paediatric patients from two clinical trials were included in the current analysis. Both trials were conducted within the context of the Leishmaniasis East Africa Platform (LEAP), and were registered with ClinicalTrials.gov: numbers NCT01067443, for the conventional regimen, and NCT02431143, for the allometric miltefosine dosing regimen.[12] The conventional dosing regimen of miltefosine is based on the linear weight-based dosing regimen (in mg/kg of body weight) derived from adult doses of miltefosine. In this trial, a dosage of 2.5 mg/kg of oral miltefosine was administered daily for a duration of 28 days. In contrast, the allometric dosing regimen was based on the previous simulation study,[15] and applied allometric scaling based on the FFM as the descriptor of body size in children, where the lean body weight is closely approximated using body weight, height and sex, further allowing a higher mg/kg dose for patients with lower body weight.[17] In this trial, daily doses between 2.7 and 3.9 mg/kg of oral miltefosine were administered for 28 days.

Ethics

For the trial with the conventional dosing regimen, ethical approval was granted by the national and local Ethics Committees in Kenya (Kenya Medical Research Institute) and Sudan (Institute of Endemic Diseases) before the trial began. Ethical approval was also granted by the London School of Hygiene and Tropical Medicine Ethics Committee. For the trial with the allometric dosing regimen, ethical approval was granted by Kenya Medical Research Institute and the Makerere University, Kampala, Uganda. The parents or legal guardians were informed of the study in their own language and provided written informed consent before trial enrolment was initiated.

Plasma sample collection and analysis

In both trials, plasma samples were nominally collected on days 0, 7, 14, 28, 56/60 and 210, while, in the allometric trial, an additional sample was taken on day 21 after initiation of treatment. The day 0 samples were drawn before the administration of miltefosine, as well as 4 or 8 h post first dose. Blood samples on other days were drawn prior to dose administration. Samples were stored at maximally −20°C in freezers at the clinical sites, during transport to Amsterdam and at the bio-analytical laboratory of the Netherlands Cancer Institute until they were analysed. When stored accordingly, miltefosine is stable in human plasma for at least 2410 days. A previously validated method of LC-MS/MS was used for drug quantification, with a lower limit of quantification of 4 ng/mL.[18] Validation of this assay indicated that miltefosine can be accurately quantified in human plasma with intra- and interassay precisions lower than 10.7% and 10.6%, respectively, and accuracies in the range of 95.1%–109%, for the lowest concentration level.[18]

Population PK analysis and model development

Software

Prior to PK analysis, the patient data were anonymized. Subsequently, data were analysed using a population approach by non-linear mixed-effects modelling iwth the first-order conditional estimation method with interaction (FOCE+I) in NONMEM (version 7.3.0, Globomax, USA)[19] using Pirana as the interface (version 2.9.6).[20] R studio (version 3.4.3) was employed for the generation of the plots used for model evaluation. All computational analyses were carried out on an internal high-performance computing cluster.

Model building

Model building was carried out in four consecutive steps according to routine procedures: (i) selection of the structural model; (ii) selection of the error model; (iii) covariate analysis; and (iv) model evaluation and validation. For the structural model, we tested both two- and three-compartment oral PK models assuming linear kinetics for absorption and elimination. Additionally, we evaluated several alternative models of absorption, such as combined zero- and first-order rates, as well as saturable absorption models. Inclusion of a lag time in all absorption models was also tested. A standard measure of model fit to the data was provided by the objective function value (OFV), expressed as minus twice the log likelihood of the data. Thus, nested hierarchical models were primarily discriminated based on their OFVs and scientific plausibility, where a decrease of 3.84 points in OFV corresponding to a P value <0.05 was considered significant, with 1 degree of freedom following χ^2 distribution. Additional goodness-of-fit criteria such as diagnostic plots, visual predictive check (VPC), standard errors of parameter estimates and inspection of the correlation matrix, as well as ε- and η-shrinkage were used in assessing the model performance. Between-subject variability (BSV) or ETAs (η, deviation of an individual parameter from the typical population value) were implemented according to equation (1). Residual unexplained variability (RUV) was explored using additive, proportional, and combined error models.

$$P_i = P_{pop} \cdot e^{\eta Pi} \quad (1)$$

where P_i is the individual parameter estimate for an individual i, and P_{pop} is the population parameter estimate, and where η^i is assumed to be distributed N (0, ω^2).

Covariate analysis

Covariate modelling was performed to identify covariates that could explain BSV, where covariates were tested univariately based on scientific plausibility. For the covariate model, various factors were considered, such as age, sex, FFM,[17] albumin levels, baseline parasite load in blood, individual *z*-scores for BMI for age, height, weight, concomitant infections and co-medication, as well as dose-derived covariates. Covariates were tested on all PK parameters according to equations 2 and 3. Exploration of potential covariate relationships was conducted by separately visualizing estimated BSV values against covariates. Calculated FFM as a descriptor of body size was included as covariate on clearance (CL/F) and volume of distribution in the central compartment (V_c/F).[21,22] Furthermore, age, sex, concomitant infections, co-medication, total cumulative dose administered in mg/day (TD) and cumulative daily dose in mg/kg/day (CD) were explored as covariates on CL, volumes of distribution of central and peripheral compartments, absorption rate constant k_a and relative oral bioavailability (F). In addition, we assessed the effects of child growth and malnutrition on F by evaluating *z*-scores for BMI for age, weight for age, and height for age in relation to decreased F in the first treatment week. AnthroPlus software developed by the WHO was used to calculate *z*-scores.[23,24] Continuous covariates were explored by various parameterizations, including both full and piece-wise covariate implementation due to observed time-associated changes in parameters as shown in the equations below. An example, equation (2), is shown for the linear model in full covariate implementation, while other functional forms such as exponential and power models were also tested. Moreover, equation (3) is a power model for piece-wise covariate implementation and, in a similar fashion, we also tested the piece-wise linear and exponential models.

$$P_{cov} = P_{pop} \cdot [1 + \theta \cdot (COV - COV_{median}) \cdot e^{\eta Pi}] \quad (2)$$

$$P_{cov} = \begin{cases} P_{pop} \cdot [(COV/COV_{threshold})^{\wedge}\theta \cdot e^{\eta Pi}] \text{ when} \geq \text{threshold} \\ P_{pop} \text{ when COV} < \text{threshold} \end{cases} \quad (3)$$

Where P_{cov} is the estimated individual parameter value for subjects who share a common covariate pattern, P_{pop} the estimated population parameter value and ηPi is the individual subject deviation from the population value for parameter P and individual i, assuming normal distribution around zero for the parameter variance in the population. COV is the tested covariate, while θ represents the estimated effect of that covariate on P_{pop}. The threshold is any value between the minimum and maximum values of the respected covariate. The piece-wise functions above assume linear relationships between the parameter and covariate until a threshold point is reached, after which a different linear relationship is applied. The final value of the threshold was chosen based on a sensitivity analysis.

Model evaluation

Parameter precision estimates were obtained through a bootstrap analysis with replacement using Perl-speaks-NONMEM (PsN, version 4.7)[25] where 1000 datasets were resampled from the original dataset to refit the model. In addition, VPCs of 1000 simulations using the final population model parameters were evaluated and stratified for each clinical trial.

Assessment of achieved exposure levels

The model developed was used to calculate individual patient estimates of secondary PK parameters, based on the predictions of their individual PK profiles. Various parameters for exposure were compared, as represented by the AUC from day 0 till the end of the first treatment week (day 7; AUC_{d0-7}), as well as until the end of the treatment (day 28; AUC_{d0-28}) and the last day of the follow-up period (day 210; AUC_{d0-210}). In addition, the time above the target and the time to reach the target were calculated,

Table 1. Patient demographics and dosing of miltefosine

	Conventional dosing regimen	Allometric dosing regimen
Miltefosine dose (mg/kg/day), median (range)	2.38 (1.25–3.33)	3.2 (2.7–3.9)
Total number of patients	21	30
Kenya	7	21
Sudan	14	—
Uganda	—	9
Sex: female (%)	24%	27%
Age (years), median (range)[a]	10 (7–12)	7 (4–12)
Body weight (kg), median (range)	24 (16–34)	21.8 (13.0–29.50)
Height (m), median (range)	1.35 (1.07–1.53)	1.25 (0.99–1.45)
FFM (kg), median (range)	20.75 (12.84–28.54)	18.16 (10.75–24.25)
BMI (kg/m^2), median (range)	13.77 (12.07–17.04)	13.66 (12.36–15.71)
z-score for BMI for age[b]	−1.87 (−3.76 to 1.01)	−1.64 (−2.93 to 2.58)
z-score for weight for height[b]	−0.95 (−3.08 to −0.36)	−1.00 (−2.23 to 0.76)
z-score for height for age[b]	−0.08 (−2.83 to 1.46)	0.08 (−1.99 to 3.07)

[a]Inclusion criteria for the minimal age differed between the trials: with the conventional dose, the youngest treated child was 7 years, and 4 years with the allometric dose.
[b]*z*-score for BMI for age was evaluated in children aged between 5 and 12 years. For children younger than 5 years, *z*-score for weight for height was used. Children younger than 5 years were considered underweight when their *z*-score was <−2 and overweight when their *z*-score was >2. Children aged between 5 and 12 years were considered underweight when their *z*-score was <−2 and overweight when their *z*-score was >1.

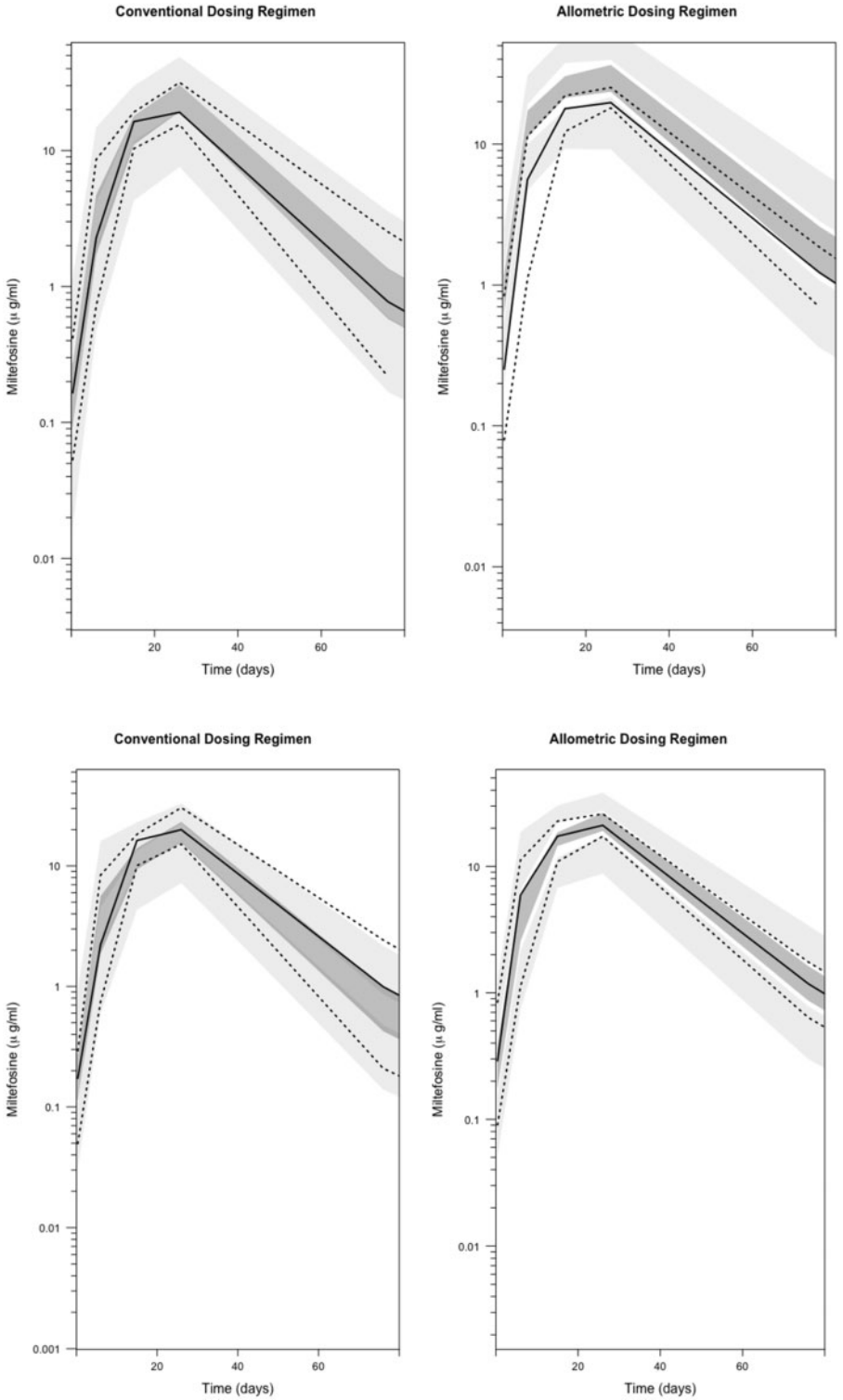

Figure 1. Prediction corrected VPCs based on 1000 simulations for the previously published PK model[14] (upper plots) as well as the newly developed model (lower plots) for the miltefosine PK in the paediatric VL patients from East Africa. The solid lines represent the median concentrations observed in each of the trials, and dark grey shading shows the simulated values. The dotted lines are representative of the 5th and 95th percentiles of the observed data, while light grey shaded areas represent the 95% CI for the simulated data.

where the target was defined as the EC_{90} equivalent to 10.6 μg/mL. This value was established by *in vitro* experiments investigating intracellular susceptibility of *Leishmania donovani* amastigotes from Eastern Africa to miltefosine.[14]

Results

Patients

Details of the patient demographics and dosing schedules are given in Table 1. Fifty-one patients were included in this population PK analysis, of which 30 were treated with oral miltefosine based on the allometric dosing regimen, and 21 based on the conventional dosing regimen. In total, 343 miltefosine plasma concentrations during and after the treatment period were available and used for building the model. Only two measurements were below the limit of quantification and were excluded from this analysis.

Structural PK model

Post-hoc individual predictions for the PK data of patients receiving the allometric regimen, based on the PK model previously developed from the conventional dosing regimen trial data,[14] showed overprediction of miltefosine accumulation in the last week of treatment as illustrated by the upper VPC plots (Figure 1). Therefore, an adjusted PK model was estimated to adequately fit the observed PK profiles of both dosing regimens (Figure 2). A two-compartment model assuming first-order absorption and linear elimination, with two separate non-linearities influencing F (Figure 3), was found to describe these data best. Parameter estimates and respective bootstrap values are given in Table 2. Similar to previous results,[13] a 69% (95% CI 61%–77%) lower F was

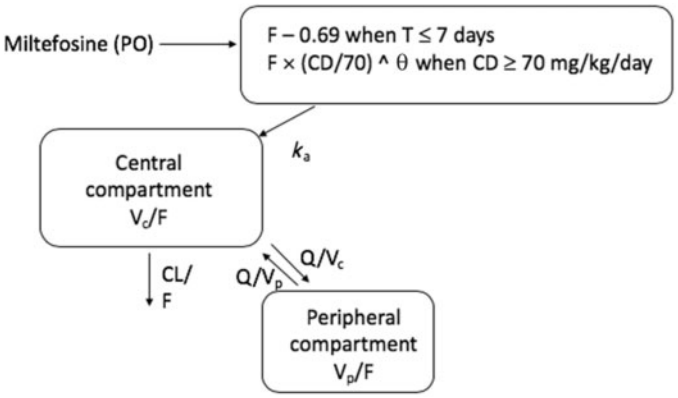

Figure 2. Schematic representation of the developed model for miltefosine PK. V_p, volume of distribution in the peripheral compartment; Q, intercompartmental clearance; T, time, θ, estimated effect of CD on F.

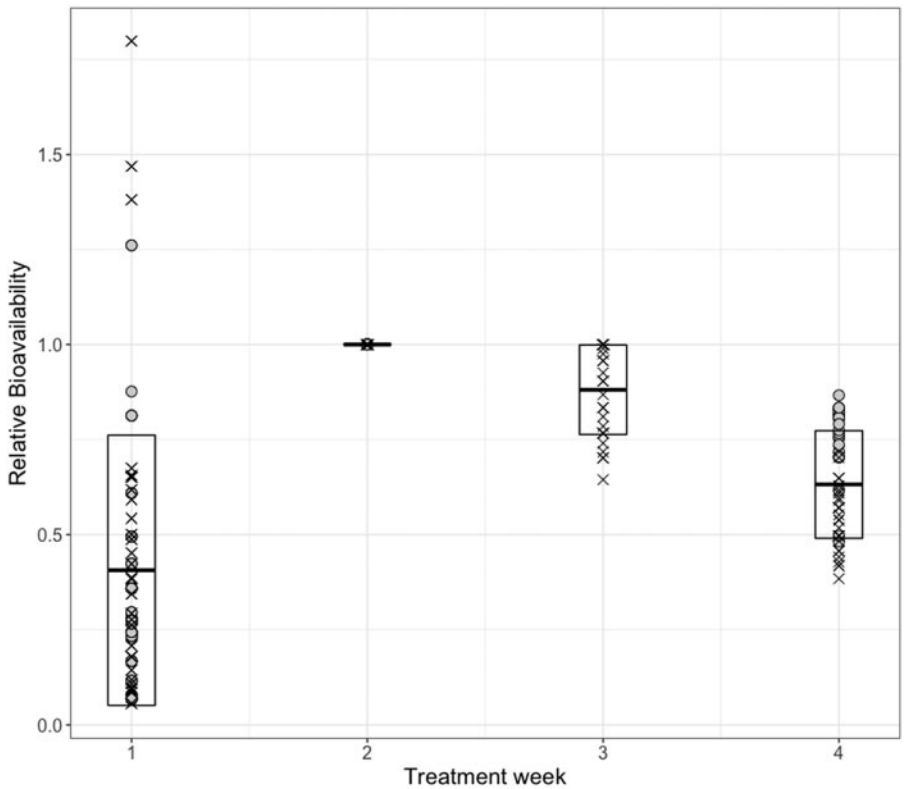

Figure 3. Miltefosine relative oral bioavailability during the course of treatment: two non-linearities described (i) a variable decrease in bioavailability during the first week of treatment (ΔOFV −223.9), most probably due to patient initial malnourishment and malabsorption, and (ii) an effect of the cumulative dose on bioavailability in the later phase of treatment (ΔOFV −22). Circles represent the estimates for individual patients treated with the conventional miltefosine regimen, while the crosses represent the same for patients treated with the allometric regimen. Error bars show the standard error of the mean.

Table 2. Parameter estimates and precisions of the final PK model

Parameter (unit)	Estimate [shrinkage %]	Bootstrap estimates[a] median (5%–95% CI)[b]
Fixed effects		
CL/F (L/day)	2.44	2.42 (2.25–2.61)
V_c/F (L)	22.9	22.8 (21.4–24.39)
k_a (day^{-1})	1.61	1.63 (1.07–2.15)
Q/F (L/day)	0.0233	0.023 (0.019–0.027)
V_p/F (L)	2.27	2.26 (2.04–2.49)
F	1 fixed	1 fixed
relative decrease F first week	−0.69	−0.69 (−0.77 to −0.61)
exponent of power relationship between CD and F[c]	−1.72	−1.69 (−2.34 to −1.11)
Between-subject variability		
CL/F (%)	19.5 [28%]	19.3 (11.4–25.1)
decreased F at treatment start (%)	86.4 [2%]	85.3 (21.7–101)
Residual unexplained variability		
proportional error (%)	37 [9%]	36.5 (10.3–40.1)

V_p, volume of distribution in the peripheral compartment; Q, intercompartmental clearance.
[a]Obtained from 665 bootstrap samples.
[b]Non-parametric CI.
[c]Applies after a CD of 70 mg/kg/day is reached, see equation (3).

estimated in the first treatment week (ΔOFV −19.4), presumably due to initial malnourishment and malabsorption. This decrease in F appeared highly variable between patients, and inclusion of BSV in this parameter improved the fit substantially (BSV 86.4%, 95%CI 21%–101%, ΔOFV −223.9). Model-based simulations as indicated in VPC plots (Figure 1, lower plots) showed a satisfactory median prediction, while the variability at the end of the treatment period was slightly overpredicted for the allometric regimen in comparison with the conventional regimen.

Covariate assessment

Evaluation of *z*-scores for BMI, height, weight, concomitant infections, parasite load at baseline or medication could not explain the variability in miltefosine PK. In addition, a retrospective evaluation of albumin plasma levels in children treated with the allometric dosing regimen indicated that only one patient had increased albumin levels between days 14 and 21, suggesting no possible explanation for the stagnation during this time period in miltefosine accumulation in plasma. Furthermore, TD and CD were examined with respect to exposure differences observed among the two dose regimens. CD implemented as a piece-wise power function (Equation 3) on F was associated with the largest ΔOFV (−11.8), compared with on CL (ΔOFV −4.5), V_c (ΔOFV −3.78) or k_a (ΔOFV −3.24). A threshold value was chosen based on a sensitivity analysis (values ranging from 10 to 110 mg/kg/day, i.e. minimum to maximum CD values throughout the treatment), which indicated that a threshold of 70 mg/kg/day was the most appropriate. Plots of the goodness of fit of the final model are shown in Figure 4. Precision of parameter estimates is given in Table 2.

PK target attainment

PK parameters reflecting achieved exposure levels at various timepoints during and after treatment were calculated for all patients using the final PK model and are provided in Table 3. The allometric dosing regimen resulted in a 1.7-fold higher exposure in the first treatment week compared with conventional therapy, with a median AUC_{d0-7} of 22 μg·day/mL versus 13 μg·day/mL for patients receiving the allometric and conventional dosing regimens, respectively. The median exposure during the treatment period (AUC_{d0-28}) was 16.4% higher for the allometric dose than for the conventional dosing regimen. The time above EC_{90} ($T > EC_{90}$) was quite similar for both dosing regimens, while the time to reach EC_{90} was 17.4% shorter for the allometric dosing regimen, where some patients had already reached the target on day 3 of treatment, while for the conventional dosing regimen no patient reached the target until day 7 (Table 3). Target achievement within the first treatment days is especially clinically meaningful given that the parasite load is highest in this period of the treatment. Nonetheless, by the end of the third treatment week, with the allometric dosing regimen 99% of the patients reached the target exposure, while 38% of the patients remained below the target with the conventional dosing regimen in the same treatment period.

Discussion

This is the first study to compare the conventional and allometric dosing regimen of miltefosine in children suffering from VL, as well as to characterize the observed non-linearities in miltefosine PK following these dosing regimens. The newly developed population PK model for miltefosine was adequate for assessing miltefosine exposure in both the conventional and allometric dosing regimens, and accounts for dose-related effects on the apparent F, previously not observed in the conventional dosing regimen. A faster achievement of the target exposure is clinically important, leading to feweer underexposed individuals, who might be more at risk for eventual treatment failure.

In addition, our model includes two separate non-linearities, accounting for both the effects of malnourishment and increased dose on miltefosine PK. Initial malabsorption by the patients at the start of treatment resulted in a 69.3% decrease in F. Food was added during miltefosine administration in both trials as much as feasible to avoid gastrointestinal side effects, which might have resulted in improved drug absorption. Furthermore, arrest of miltefosine accumulation in the third week of treatment was observed in 40% of the children treated with the allometric dose. Considering the 28% median increase in the dose in the allometric trial, exposure was lower than initially anticipated according to dose proportionality. The median plasma concentration at the end of treatment was 20.9 μg/mL compared with the earlier model-predicted concentration of 29.7 μg/mL. As a result, children who received the allometric dose still had lower exposure compared with that observed in adults after conventional dosing.[16] Patient populations in both trials share demographic characteristics and

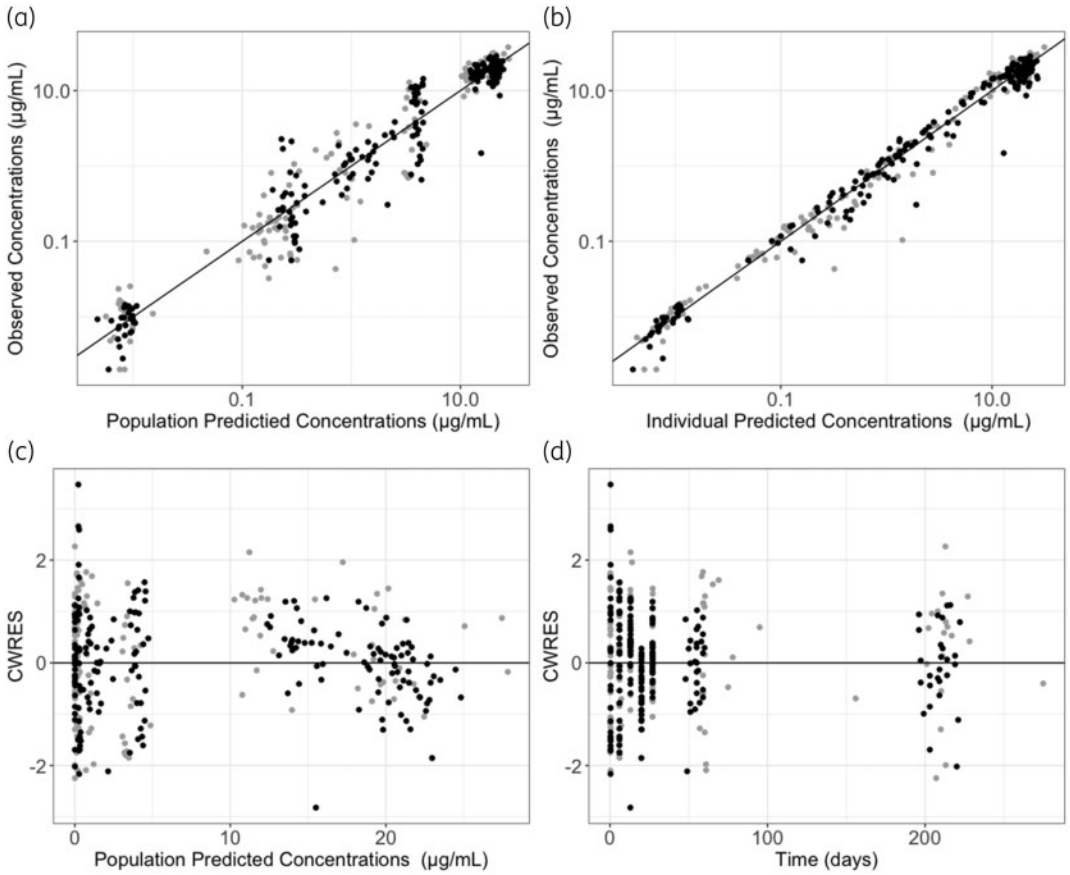

Figure 4. Goodness-of-fit plots for the final PK model depicting both data from the allometric (grey) and conventional dosing (black) regimens. (a) Observed versus population predicted miltefosine concentrations, (b) observed versus individually predicted miltefosine concentrations, (c) conditional weighted residuals (CWRES) versus population predicted concentrations and (d) CWRES versus time after start of treatment.

Table 3. Individual model-based estimates of the miltefosine exposure and target attainment

	Conventional dosing regimen		Allometric dosing regimen	
Exposure parameter (unit)	median	range	median	range
AUC_{d0-7} (µg·day/mL)	13.00	3.07–42.87	22.85	4.14–96.02
AUC_{d0-28} (µg·day/mL)	321.9	261.2–478.0	385.5	271.0–651.7
AUC_{d0-210} (µg·day/mL)	550.5	404.1–891.6	588.6	396.0–875.7
$T > EC_{90}$ (days)	23.4	17–32.3	24.5	17.46–33.3
Time to reach EC_{90} (days)	12.21	6.44–14.15	10.26	2.51–13.41

there were no observed differences between sex or age. Other factors potentially influencing the credibility of the observed miltefosine concentrations could be excluded, since sampling and transport procedures were the same in the two separate trials, as well as procedures regarding sample preparation and quantification of the analyte in the laboratory. Therefore, we evaluated whether *z*-scores for BMI, height, weight, albumin levels, concomitant infections or medication during the treatment with miltefosine could have potentially led to the observed halt in miltefosine accumulation in the last weeks of treatment, but no differences were found in the dynamics of these factors between patients receiving either dosing regimen.

Next, we evaluated dosing-related covariates TD and CD on all PK parameters of interest, using various parameterizations. We established that a reduction of miltefosine F with an increasing CD above 70 mg/kg/day best explained the arrest in miltefosine accumulation in the third week of treatment in the allometric dosing regimen. A possible explanation for this phenomenon could be the slow and saturable transcellular transport of miltefosine over the gastrointestinal membrane.[9] *In vitro* studies have previously

suggested the involvement of saturable processes of absorption for miltefosine and the incorporation of miltefosine in the cellular membrane lipid bilayer.[8,9,26,27] This is corroborated by the slow oral absorption rates for miltefosine that have been estimated in various population PK studies, including this one.[7,13,22] Data sparseness in the absorption phase prevented more mechanistic parameterizations of potential distinction between absorption by passive diffusion at low concentrations and saturable processes after higher concentrations accumulated in plasma, although some attempts were made (see the Methods). Nevertheless, the estimated k_a in this study indicated very slow absorption kinetics, which is in line with previous studies.[7,14] Extrapolations using this model outside of the observed dosing range should be performed with great caution, given the non-mechanistic nature of the relationship between CD and miltefosine bioavailability.

In addition, with the increase in dose in the allometric regimen, safety profiles observed were comparable to those with the conventional regimen. With the allometric regimen, 43% of patients experienced treatment-emerging adverse effects, such as gastrointestinal disorders, commonly related to treatment with miltefosine, also in adults, but none of the patients discontinued treatment due to an adverse effect,[16] which is comparable to the conventional regimen.[12]

In conclusion, this study characterized the dose-related non-linearities in miltefosine PK. Adequate early exposure to miltefosine is of critical importance for treatment response, due to the highest parasite load in this period. Regardless of the unforeseen lack of dose proportionality for miltefosine exposure during treatment with the allometric dosing regimen, the nearly doubled miltefosine exposure in the first week, which led to fewer underexposed individuals and earlier and higher PK target attainment, potentially resulted in the observed improved treatment efficacy, which increased from 59% for the conventional miltefosine regimen to 90% for the allometric regimen (95% CI 73%–98%). This study, therefore, highlights the importance of adopting an allometric weight-based dosing schedule for miltefosine treatment of VL in paediatric patients.

Acknowledgements

We sincerely thank the VL patients and their parents/guardians for their willingness to be enrolled in the studies on which this work is based and for their cooperation. We would also like to recognize the professional technical and logistical support from the clinical study teams and laboratory technicians at the clinical sites in Kacheliba and Kimalel (Kenya), in Amudat (Uganda), and in Dooka and Kassab (Sudan). Furthermore, we would like to thank the Drugs for Neglected Diseases *initiative* (DND*i*). Africa Data Center for their assistance. This study was conducted within the Leishmaniasis East Africa Platform (LEAP) and was coordinated and funded by the DND*i*. Lastly, we thank Louise Burrows for reviewing of this manuscript, and the Research HPC facility of the Netherlands Cancer Institute for support in the use of computational resources.

Funding

This work was supported through the DND*i* by the European Union Seventh Framework Programme (FP7) Africoleish (grant number 305178); the WHO—Special Programme for Research and Training in Tropical Diseases (WHO-TDR); the French Development Agency (AFD), France (grant CZZ2062); UK Aid, UK; the Federal Ministry of Education and Research (BMBF) through KfW, Germany; the Medicor Foundation Liechtenstein; Médecins Sans Frontières (MSF) International; the Swiss Agency for Development and Cooperation (SDC), Switzerland (grant 81017718); the Dutch Ministry of Foreign Affairs (DGIS), the Netherlands (grant PDP15CH21); the French Ministry for Europe and Foreign Affairs (MEAE), France; the Spanish Agency for International Development Cooperation (AECID), Spain; and other private individuals and foundations. T.P.C.D. is personally supported by the ZonMw/Dutch Research Council (NWO) Veni grant (project no. 91617140).

Transparency declarations

None to declare.

References

1 Alvar J, Vélez ID, Bern C *et al.* Leishmaniasis worldwide and global estimates of its incidence. *PLoS One* 2012; **7**: e35671.

2 Boelaert M, Meheus F, Sanchez A *et al.* The poorest of the poor: a poverty appraisal of households affected by visceral leishmaniasis in Bihar, India. *Trop Med Int Heal* 2009; **14**: 639–44.

3 Kedzierski L, Sakthianandeswaren A, Curtis JM *et al.* Leishmaniasis: current treatment and prospects for new drugs and vaccines. *Curr Med Chem* 2009; **16**: 599–614.

4 Chappuis F, Sundar S, Hailu A *et al.* Visceral leishmaniasis: what are the needs for diagnosis, treatment and control? *Nat Rev Microbiol* 2007; **5**: S7–16.

5 Dorlo TPC, Balasegaram M, Beijnen JH *et al.* Miltefosine: a review of its pharmacology and therapeutic efficacy in the treatment of leishmaniasis. *J Antimicrob Chemother* 2012; **67**: 2576–97.

6 Bianciardi P, Brovida C, Valente M *et al.* Administration of miltefosine and meglumine antimoniate in healthy dogs: clinicopathological evaluation of the impact on the kidneys. *Toxicol Pathol* 2009; **37**: 770–5.

7 Dorlo TPC, van Thiel P, Huitema ADR *et al.* Pharmacokinetics of miltefosine in Old World cutaneous leishmaniasis patients. *Antimicrob Agents Chemother* 2008; **52**: 2855–60.

8 Ménez C, Buyse M, Dugave C *et al.* Intestinal absorption of miltefosine: contribution of passive paracellular transport. *Pharm Res* 2007; **24**: 546–54.

9 Ménez C, Buyse M, Farinotti R *et al.* Inward translocation of the phospholipid analogue miltefosine across Caco-2 cell membranes exhibits characteristics of a carrier-mediated process. *Lipids* 2007; **42**: 229–40.

10 Sundar S, Jha T, Sindermann H *et al.* Oral miltefosine treatment in children with mild to moderate Indian visceral leishmaniasis. *Pediatr Infect Dis J* 2003; **22**: 434–8.

11 Sundar S, Jha TK, Thakur CP *et al.* Oral miltefosine for Indian visceral leishmaniasis. *N Engl J Med* 2002; **347**: 1739–46.

12 Wasunna M, Njenga S, Balasegaram M *et al.* Efficacy and safety of AmBisome in combination with sodium stibogluconate or miltefosine and miltefosine monotherapy for African visceral leishmaniasis: phase II randomized trial. *PLoS Negl Trop Dis* 2016; **10**: e0004880.

13 Dorlo TPC, Rijal S, Ostyn B *et al.* Failure of miltefosine in visceral leishmaniasis is associated with low drug exposure. *J Infect Dis* 2014; **210**: 146–53.

14 Dorlo TPC, Kip AE, Younis BM *et al.* Visceral leishmaniasis relapse hazard is linked to reduced miltefosine exposure in patients from Eastern Africa: a population pharmacokinetic/pharmacodynamic study. *J Antimicrob Chemother* 2017; **72**: 3131–40.

15 Dorlo TPC, Huitema ADR, Beijnen JH *et al.* Optimal dosing of miltefosine in children and adults with visceral leishmaniasis. *Antimicrob Agents Chemother* 2012; **56**: 3864–72.

16 Mbui J, Olobo J, Omollo R *et al*. Pharmacokinetics, safety and efficacy of an allometric miltefosine regimen for the treatment of visceral leishmaniasis in Eastern African children: an open-label, phase-II clinical trial. *Clin Infect Dis* 2019; **68**: 1530–8.

17 Al-Sallami HS, Goulding A, Grant A *et al*. Prediction of fat-free mass in children. *Clin Pharmacokinet* 2015; **54**: 1169–78.

18 Dorlo TPC, Hillebrand MJX, Rosing H *et al*. Development and validation of a quantitative assay for the measurement of miltefosine in human plasma by liquid chromatography–tandem mass spectrometry. *J Chromatogr B* 2008; **865**: 55–62.

19 Keizer RJ, Karlsson MO, Hooker A. Modeling and simulation workbench for NONMEM: tutorial on Pirana, PsN, and Xpose. *CPT: Pharmacomet Syst Pharmacol* 2013; **2**: e50.

20 Keizer RJ, van Benten M, Beijnen JH *et al*. Piraña and PCluster: a modeling environment and cluster infrastructure for NONMEM. *Comput Methods Programs Biomed* 2011; **101**: 72–9.

21 Janmahasatian S, Duffull SB, Ash S *et al*. Quantification of lean bodyweight. *Clin Pharmacokinet* 2005; **44**: 1051–65.

22 Kip AE, Castro M del M, Gomez MA *et al*. Simultaneous population pharmacokinetic modelling of plasma and intracellular PBMC miltefosine concentrations in New World cutaneous leishmaniasis and exploration of exposure–response relationships. *J Antimicrob Chemother* 2018; **73**: 2104–11.

23 WHO. Application Tools: AnthroPlus Software. https://www.who.int/growthref/tools/en/.

24 WHO. *Global Database on Child Growth and Malnutrition*. https://www.who.int/nutgrowthdb/en/.

25 Lindbom L, Ribbing J, Jonsson EN. Perl-speaks-NONMEM (PsN)—a Perl module for NONMEM related programming. *Comput Methods Programs Biomed* 2004; **75**: 85–94.

26 Malta de Sá M, Sresht V, Rangel-Yagui CO *et al*. Understanding miltefosine–membrane interactions using molecular dynamics simulations. *Langmuir* 2015; **31**: 4503–12.

27 Barratt G, Saint-Pierre-Chazalet M, Loiseau PM. Cellular transport and lipid interactions of miltefosine. *Curr Drug Metab* 2009; **10**: 247–55.